Nonuniversal gaugino masses, the supersymmetric little hierarchy problem, and dark matter

James E. Younkin and Stephen P. Martin

Phys. Rev. D **85**, 055028 — Published 30 March 2012

DOI: 10.1103/PhysRevD.85.055028

Non-universal gaugino masses, the supersymmetric little hierarchy problem, and dark matter

James E. Younkin[1] and Stephen P. Martin[1,2]

[1] *Department of Physics, Northern Illinois University, DeKalb IL 60115 and*

[2] *Fermi National Accelerator Laboratory, P.O. Box 500, Batavia IL 60510*

We study a class of supersymmetric models with non-universal gaugino masses that could arise from F-terms in a general combination of the singlet and adjoint representations of $SU(5)$. We explore models that satisfy present Large Hadron Collider and other bounds, showing how the allowed parameter space is divided into distinct "continents". Regions of parameter space that ameliorate the supersymmetric little hierarchy problem with a small μ parameter include the usual focus point scenario, but also natural areas with much lighter squarks and sleptons. These models are continuously connected in parameter space to regions in which stau co-annihilation or Higgs exchange is mostly responsible for dark matter annihilation, and to models in which the thermal relic abundance is achieved by slepton-mediated annihilation, reviving the bulk region that is severely restricted in mSUGRA models. In hybrid or confluence regions, several mechanisms combine to give the requisite dark matter annihilation rate. In each case we study the prospects for direct detection of dark matter. We also comment briefly on the impact of recent hints for M_h near 125 GeV from the LHC.

I. INTRODUCTION

Supersymmetry [1] as an extension of the Standard Model (SM) provides a way of explaining why the weak scale is so small compared to the Planck scale or other very high energy scales in fundamental physics. The Large Hadron Collider (LHC) is presently engaged in searches with increasing sensitivity to supersymmetry [2, 3], excluding significant areas of parameter space corresponding to lower gluino and up-squark and down-squark masses. Searches by underground detectors for a stable neutralino lightest supersymmetric particle (LSP) as the dark matter are also probing interesting parts of parameter space [4, 5]. In addition, the non-observation of a Higgs boson at the CERN LEP e^+e^- collider [6] places a very non-trivial constraint on the supersymmetric models. These searches increase the lower bounds on superpartner masses, leading to an apparent fine-tuning problem known as the supersymmetric little hierarchy problem. The essence of this problem is the tension between the Z boson squared mass and the much larger soft supersymmetry-breaking squared masses.

In the Minimal Supersymmetric Standard Model (MSSM), this problem can be understood by considering the relationship between input parameters and the electroweak scale, which may be written as

$$m_Z^2 = -2(|\mu|^2 + m_{H_u}^2) + \dots \tag{1.1}$$

where the ellipses denote loop correction effects (which can be made small by an appropriate choice of renormalization scale) and a tree-level contribution suppressed by $1/\tan^2\beta$. Here $\tan\beta$ is equal to the ratio of Higgs expectation values $\langle H_u\rangle/\langle H_d\rangle$, μ is the superpotential Higgs mass parameter, and $m_{H_u}^2$ is the soft supersymmetry breaking squared mass of the Higgs boson that couples to the top quark. The cancellation needed between $|\mu|^2$ and $m_{H_u}^2$ may therefore be regarded as an indication[†] of the fine-tuning required to obtain the observed weak scale.

In terms of the input running gaugino masses M_1, M_2, M_3 at the apparent unification scale $M_U = 2\times 10^{16}$ GeV, one finds from running two-loop renormalization group equations [7] that $m_{H_u}^2$ at the TeV scale is approximately:

$$\begin{aligned} -m_{H_u}^2 \;=\; & 1.82M_3^2 - 0.21M_2^2 + 0.16M_3M_2 + 0.023M_1M_3 + 0.006M_1M_2 - 0.006M_1^2 \\ & -0.32A_0M_3 - 0.07A_0M_2 - 0.022m_0^2. \end{aligned} \tag{1.2}$$

[†] Because there is no objective measure on parameter space, we do not attempt any detailed quantification of fine-tuning, but do view it as a qualitatively valid motivation and concern.

Here we have chosen $\tan\beta = 10$ and chosen flavor-blind scalar squared masses m_0^2 and a universal scalar cubic coupling parameter A_0 for illustration. In the subspace of models with unified gaugino masses $M_1 = M_2 = M_3 = m_{1/2}$ at M_U (often referred to as either "mSUGRA" or "CMSSM" in the literature), lower bounds on the gluino mass imply a significant fine tuning in order to reconcile equations (1.1) and (1.2). This will worsen if the LHC sets new limits, a plausible prospect in the very near future.

This motivates models with non-universal gaugino masses, in particular those in which the gluino mass parameter M_3 is relatively small compared to the wino mass parameter M_2. As can be seen from eq. (1.2), a small ratio of M_3/M_2 can lower $-m_{H_u}^2$ and therefore decrease the amount of cancellation needed with $|\mu|^2$ [8]. In this paper, we will explore some features, including dark matter properties, of a class of non-universal gaugino mass models, with particular attention to models that can naturally accommodate small $|\mu|$ and are therefore more attractive from the perspective of the supersymmetric little hierarchy problem.

Specifically, we will use a class of models that have the gauginos getting contributions to their masses from an F-term that transforms as a **24** representation of the global $SU(5)$ group that contains the SM gauge group [9]. This yields a contribution to the gaugino masses in the ratio $M_1 : M_2 : M_3 = 1 : 3 : -2$. The same pattern arises [10] if the F-terms transform as a **54** representation of the global $SO(10)$ group that contains $SU(5)$. In either case, the group may or may not be promoted to a true grand unification gauge group. Gaugino masses in this pattern may be added to a universal contribution $M_1 : M_2 : M_3 = 1 : 1 : 1$.

In the CMSSM, there are four main mechanisms that allow for dark matter annihilation that is efficient enough to prevent the early universe from becoming matter dominated too soon. First, the "bulk" region at small m_0 and small $m_{1/2}$ allows efficient dark matter annihilation by t-channel slepton exchange. This region is under considerable pressure (if not eliminated entirely) by the LEP and LHC bounds, but with gaugino mass non-universality we will see that it is easily resurrected. Second, there is a co-annihilation region at small m_0, in which the lightest stau co-exists and co-annihilates in the early universe with an LSP that is not much lighter [11]. Third, a "focus point" or "small μ" region [12] at very large m_0, has μ small, so that mostly bino-like LSPs contain a subdominant but significant Higgsino admixture, allowing them to annihilated efficiently [12] to and through weak bosons. If the LSP mass exceeds m_t, then the final state of dark matter pair annihilations can be $t\bar{t}$ in this case. Fourth, at large $\tan\beta$ the A^0-funnel region allows the LSPs to annihilate through s-channel pseudo-scalar Higgs exchange [13]. In the more general MSSM, there is also a possibility of LSPs that co-annihilate efficiently because they are wino-like [14], but this

cannot be realized in the unified gaugino mass case. In the following, we will take the dark matter density to be in the conservative range

$$0.09 < \Omega_{\rm DM} h^2 < 0.13, \tag{1.3}$$

where $h \approx 0.71$ is the Hubble parameter today in units of km/(sec Mpc). It is very important that it is optional to require the predicted thermal relic abundance to lie in this range, because there are a variety of easy ways to evade this bound (see for example [15]). If the predicted $\Omega_{\rm DM} h^2$ for a particular model comes out lower than 0.09, then axions or some other species could make up the difference, and so this region of parameter space should not be viewed as disallowed. If $\Omega_{\rm DM} h^2 > 0.13$, then one can reduce the predicted density by having the apparent LSP decay to a lighter singlet particle, or by invoking R-parity violation so that there is no supersymmetric dark matter at all. Still, it is interesting to consider the range eq. (1.3) as providing a minimal accommodation of astrophysical and cosmological observations [16].

Modifying the universal boundary conditions of CMSSM can lead to interesting new conditions for dark matter; see for some recent examples [17]-[29] and references therein. In [30], it was suggested that with a mixture of the two gaugino mass patterns mentioned above, chosen to make μ smaller, the LSP remains mostly bino-like but the observed thermal relic abundance of dark matter may be naturally obtained by efficient annihilations $\tilde{N}_1 \tilde{N}_1 \to t\bar{t}$ through t-channel exchange of top squarks. In these "compressed supersymmetry" models, the ratio of the masses of the heaviest and lightest superpartners is reduced and $|\mu|$ is also much smaller than encountered in the CMSSM. However, only models continuously connected in parameter space to the CMSSM case were considered in [30]. In this paper, we will study the full parameter space obtained by varying over the entire allowed range spanned by linear combinations of the two gaugino mass contribution patterns $M_1 : M_2 : M_3 = 1 : 1 : 1$ and $1 : 3 : -2$. The viable parameter space is typically divided into three separate "continents", with distinctive features. In the following, we will characterize these regions in terms of the size of the μ parameter, and in terms of the mechanisms that can allow the dark matter abundance to be in approximate agreement with cosmological observations. In the larger parameter space spanned by non-zero F terms in the **24** of $SU(5)$, the dark-matter allowed regions mentioned above merge and are deformed in interesting ways. One of the more interesting scenarios is a parameter-space region with small $|\mu|$ that is continuously connect to the CMSSM focus-point region, but occurs at much lower values of m_0 when gaugino-mass non-universality is significant. There are similar regions that are not continuously connected to the CMSSM focus point region. There are also stau co-annihilation and bulk regions, some of which are

not continuously connected to the corresponding CMSSM regions, and which have very different prospects for dark matter direct detection. We will also discuss an intriguing viable region formed by a confluence between the A^0-funnel, small-μ, and stau co-annihilation regions, which can occupy a large chunk of parameter space, and which we refer to as the confluence island. However, this region is severely impacted by indirect constraints, as we will see.

II. PARAMETERIZATIONS AND CONSTRAINTS

In this paper, we will parameterize a general combination of the universal and non-universal gaugino mass patterns mentioned in the Introduction in terms of an overall gaugino mass scale $m_{1/2}$ and an angle θ_{24}, which we define as:

$$M_1 = m_{1/2}\left(\cos\theta_{24} + \sin\theta_{24}\right), \tag{2.1}$$

$$M_2 = m_{1/2}\left(\cos\theta_{24} + 3\sin\theta_{24}\right), \tag{2.2}$$

$$M_3 = m_{1/2}\left(\cos\theta_{24} - 2\sin\theta_{24}\right). \tag{2.3}$$

Note that $\theta_{24} = 0$ corresponds to the usual unified gaugino mass scenario, while $\theta_{24} = \pm\pi/2$ correspond to a pure **24** of $SU(5)$ [or **54** of $SO(10)$] F term contribution. Taking $\theta_{24} \to \theta_{24} + \pi$ flips the signs of all three gaugino masses simultaneously, which is physically the same as the original model with the signs of the scalar cubic couplings and μ term flipped.

Because of the high dimensionality of parameter space, it is not possible to do a complete study, and some choices must always be made in order to illustrate qualitative features. In this paper, we choose to include only a universal scalar squared mass m_0^2, despite the fact that non-universal gaugino masses might be expected to be accompanied by non-universality of some kind in the scalar sector. We assume this scalar mass non-universality to be small, or that it would lead to qualitative features similar to the results we obtain, but it would certainly be interesting to consider alternatives. In this regard, note that the scalar soft squared masses will arise in the form $F^*F/M^2_{\rm Planck}$, which transform in the product of the representation R_F of F and its conjugate, R_F^*. The direct product representation $R_F \times R_F^*$ will always include the $SU(5)$ [or $SO(10)$] singlet representation, so that it is sensible to take a common m_0^2, but it also can include other non-trivial GUT representations. Therefore, it would be just as reasonable to explore other patterns, but we will not do so here. The parameters m_0 and θ_{24}/π will be varied independently.

In our explorations of parameter space, we used `SOFTSUSY 3.1.2` [31] to generate supersymmet-

ric spectra,[†] using $m_t = 173.3$ GeV, $M_b(M_B)^{\overline{\rm MS}} = 4.25$ GeV, and $\alpha_S(M_Z) = 0.118$. The program `micrOMEGAs 2.2` [33] was used to evaluate dark matter thermal relic abundance, the LSP-nucleon cross-section for dark matter detection, and implement constraints from other observables as follows. For $B \to \tau\nu$ mediated by charged Higgs bosons, we follow [34] by taking a constraint

$$m_{H^+} > 13.5 \tan\beta. \tag{2.4}$$

We also consider a constraint

$$\mathrm{BR}(B_s \to \mu^+\mu^-) < 1.1 \times 10^{-8} \tag{2.5}$$

from [35]. There is a well-known deviation of the anomalous magnetic moment of the muon measured by [36] from the Standard Model predicted values. Since we are unwilling to interpret this measurement as ruling out the Standard Model, we follow the "super-conservative" attitude of [37] by only requiring agreement within 5σ:

$$-2.5 \times 10^{-9} < \Delta a_\mu < 6.5 \times 10^{-9} \tag{2.6}$$

Here Δa_μ is the supersymmetric contribution to $(g_\mu - 2)/2$. In the models we consider, this only impacts the very high $\tan\beta$ case. For $b \to s\gamma$, we implement a constraint

$$2.0 \times 10^{-4} < \mathrm{BR}(b \to s\gamma) < 5.0 \times 10^{-4}, \tag{2.7}$$

which is also somewhat more conservative than commonly imposed [38]. This is because constraints on the supersymmetric contribution to this observable only apply if one accepts the additional assumption of minimal flavor violation in the soft supersymmetry-breaking sector. Because there is no reason not to expect additional sources of flavor violation, this constraint should not be considered mandatory. One could even adopt the point of view that no strict $\mathrm{BR}(b \to s\gamma)$ limit applies at all, although relying on non-minimal flavor violation to counteract the minimal flavor violating contribution might be seen as requiring some fortuitous tuning. In the models encountered below, h^0 has couplings very close to those of a Standard Model Higgs boson, but we use a slightly lower bound than the Standard Model 114.4 GeV LEP bound because of theoretical uncertainties in the mass prediction in supersymmetry; we take

$$m_{h^0} > 113 \text{ GeV}. \tag{2.8}$$

[†] In some cases, especially at high $\tan\beta$ and large m_0, we found significant numerical differences between the model calculator we used, `SOFTSUSY`, and an alternative, `SuSpect` [32], evidently due to high sensitivity of the spectrum to the particular treatment of radiative corrections and translation of input parameters into physical masses. However, we expect the qualitative features to remain robust.

All of the constraints mentioned above are implemented as contours in plots, rather than by removing the models from consideration, so that the impact of these indirect observables on the parameter space can be judged by the reader. Finally, we note that the CMS and ATLAS collaborations have announced significant limits [2, 3] on gluino and squark production, although only in the context of unified gaugino mass models and other simplified models with large hierarchies between the gluino and LSP masses. Most of the models we will study evade the LHC limits by taking sufficiently heavy gluinos, with M_3 held fixed. In cases where M_1 is held fixed instead, we will also plot the contours for $m_{\tilde{q}} = 800$ and 1000 GeV for the average squark mass on graphs below, as a very rough indication of where the exclusion reach of present LHC data might lie. However, because the superpartner mass spectrum is compressed in many of the parameter space regions we study, and the reach of the LHC can be significantly reduced in such cases [39], a true exclusion would require a dedicated study that is beyond the scope of this paper.

III. EXPLORATIONS WITH FIXED M_3

In this section, we study several slices of parameter space with M_3 held fixed at 600 GeV, so that the gluino mass is beyond the present reach of the LHC, in the range $1350 < M_{\tilde{g}} < 1525$ depending on the masses of squarks (which contribute to the gluino mass in loop corrections [40]). We will consider both moderate and large $\tan\beta$, and varying m_0 and θ_{24}. From eqs. (2.1)-(2.3), one has:

$$M_1 \,=\, M_3 \left(\frac{1+\tan\theta_{24}}{1-2\tan\theta_{24}}\right), \qquad M_2 \,=\, M_3 \left(\frac{1+3\tan\theta_{24}}{1-2\tan\theta_{24}}\right). \tag{3.1}$$

Since we are holding M_3 fixed in this section, $|M_1|$ becomes very small when θ_{24}/π approaches $-1/4$ and $3/4$. Therefore, in the graphs below we take the range for θ_{24}/π from $-1/4$ to $3/4$; this range (rather than, say, 0 to 1, or $-1/2$ to $1/2$) avoids splitting up the continents of viable parameter space in unnatural ways. At $\theta_{24}/\pi \approx -0.102$, one has M_2 approaching 0, so models near this vertical line in figures below are excluded by LEP2 limits on charginos [38], providing an ocean between the two continents. At $\theta_{24}/\pi \approx 0.148$, one has $|M_1|$ and $|M_2|$ diverging without bound, so models near this vertical line are likewise excluded, providing another gap between the two continents of viable parameter space on either side. The boundaries of the continents on either side of this line are actually determined by the fact that small $|M_3/M_2|$ leads to small $|\mu|^2$, as can be seen from eqs. (1.1) and (1.2).

This is illustrated in Figure 1, which maps the viable regions of parameter space in the (θ_{24}, m_0)

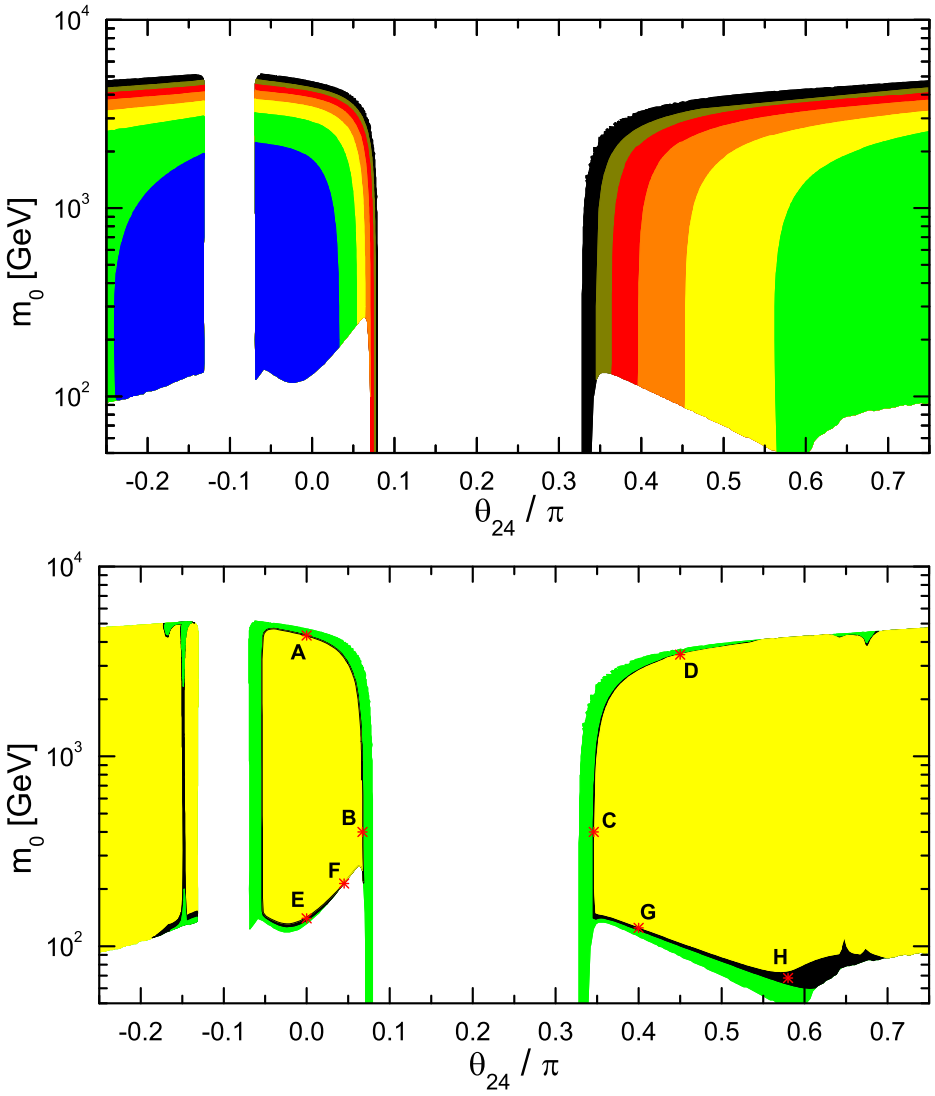

FIG. 1: Maps of the μ parameter (upper plot) and the predicted thermal relic abundance of dark matter $\Omega_{\rm DM}h^2$ (lower plot) in the θ_{24}, m_0 parameter space with fixed $M_3 = -A_0 = 600$ GeV, $\tan\beta = 10$, and $\mu > 0$. In the upper plot, the dark (black) regions at the top and closest to the center represents $\mu < 300$ GeV, and successive regions lower and away from the center correspond to 300 GeV $< \mu <$ 400 GeV (brown) and 400 GeV $< \mu <$ 500 GeV (red) and so on up to the last region (blue) which corresponds to 800 GeV $< \mu <$ 900 GeV. The regions left blank do not have viable electroweak symmetry breaking, do not have a neutralino as the LSP, or have superpartners that are too light, as described in the text. In the lower plot, the thin dark regions (black) correspond to the observed range $0.09 < \Omega_{\rm DM}h^2 < 0.13$. The large interior regions (yellow) correspond to $\Omega_{\rm DM}h^2 > 0.13$, while the darker shaded exterior region (green) has $\Omega_{\rm DM}h^2 < 0.09$.

plane, for fixed $M_3 = -A_0 = 600$ GeV, $\tan\beta = 10$, and $\mu > 0$. The choices of A_0 and $\tan\beta$ are motivated by the need to obtain a lightest Higgs mass above the LEP bound, and indeed all of the indirect bounds eq. (2.4)-(2.8) are satisfied throughout the shaded regions shown. Regions

left blank do not have viable electroweak symmetry breaking, do not have a neutralino as the LSP, or have charged superpartners (staus or charginos) that are below the LEP2 bounds [38]. The lower boundaries of the allowed continents in Figure 1, and similar figures below, are set by the requirement that the LSP is a neutralino and not a stau, as required for a supersymmetric explanation of the dark matter. The upper boundaries come from the requirement of proper electroweak symmetry breaking with positive $|\mu|^2$ in the scalar potential. On the outside parts of the plots, $-0.25 < \theta_{24}/\pi \lesssim -0.16$ and $0.66 \lesssim \theta_{24} < 0.75$, the LSP mass will be below $m_Z/2$.

The top plot in Figure 1 is a map of the μ parameter, with lower values arguably corresponding to less fine-tuning, as described in the Introduction. Note that the MSSM corresponds to the vertical line $\theta_{24} = 0$. On that line, the smallest values of μ occur at the largest allowed values of the scalar masses, near $m_0 = 4300$ GeV; this is the focus point solution. For smaller values of m_0, the solution for electroweak symmetry breaking gives larger values of μ, but it never exceeds 900 GeV throughout the whole plot. The focus point region is continuously connected to a small-μ region near $\theta_{24}/\pi = 0.65$ with a wide range of m_0 values. This region connects to a region where $\Omega_{\rm DM}h^2 < 0.09$ which extends down to very low values of $m_0 < 100$ GeV. These models survive the requirement of a neutral (non-stau) LSP because here $\mu < M_1, M_2$, so that the LSP is a higgsino-like state that is much lighter than the sleptons.

The left continent in Figure 1 corresponds to $M_2/M_3 < 0$, and contains small-μ regions only at large values of m_0, comparable to the CMSSM focus point. Recall that the far left of the plot corresponds to very light bino-like neutralino LSPs, and that the region is separated from the central, CMSSM-like continent by a region where M_2 is too small, leading to charginos below the LEP bound. The boundaries of that region are very nearly vertical, because the chargino mass depends only very weakly on m_0 through loop effects.

The right continent in Figure 1 has both M_1/M_3 and M_2/M_3 negative, and is separated from the central CMSSM-like continent by a region where $|M_2/M_3|$ is very large, as discussed above. In fact, the region from $0.08 \lesssim \theta_{24}/\pi \lesssim 0.33$ is excluded because $-m^2_{H_u}$ is negative at the TeV scale, precluding electroweak symmetry breaking. The top edge of this continent is again a small-μ focus point-like region, and the left edge of the continent near $\theta_{24}/\pi = 0.35$ also has small μ over a large range of m_0. In fact, one can see from the plot that the range of parameters over which μ is small is considerably broader than the corresponding region on the central CMSSM-like continent, so that arguably this region is less fine-tuned in producing correct electroweak symmetry breaking.

The lower plot of Figure 1 shows the same regions, but now indicating whether the predicted thermal relic abundance of dark matter is larger, smaller, or within the range of eq. (1.3). The

region where eq. (1.3) is satisfied is quite thin; this does not reflect any fine-tuning, but rather the fact that the dark matter relic abundance is now quite precisely known from experiment. In the central continent, the interior predicts too much dark matter, due to inefficient annihilation, while on the boundary there is too little dark matter. For the CMSSM at $\theta_{24} = 0$, the two allowed possibilities are the focus point region near $m_0 = 4325$ GeV and the stau co-annihilation region near $m_0 = 140$ GeV. The top and bottom edges of the central continent share these features. The vertical left edge of this continent has efficient wino co-annihilations; because of small M_2 the LSP has a significant wino content. The right edge achieves the correct dark matter abundance due to having a significant higgsino content of the LSP because μ is small, similar to the focus point case. Note that these regions are actually continuously connected, with hybrid features at the corners.

In the right continent of Figure 1, the top and left edges again have small μ. The bottom region is stau-coannihilation up to about $\theta_{24} = 0.58$, where it continuously merges into a fatter "bulk region", characterized not by stau coannihilations but by slepton-mediated annihilations to leptons. Note that the stau-coannihilation region has μ between about 300 GeV and 700 GeV, while the bulk region has μ between 700 and 800 GeV. Also visible as two small peaks are h^0-resonance [41] and Z^0 resonance regions near $\theta_{24}/\pi = -0.15$ and -0.17 respectively. The bulk region points at small m_0 on the right have light slepton masses not far above their LEP2 bounds. For the left continent of Figure 1, the h^0 resonance region cuts vertically through the entire continent, connecting to small-μ and bulk regions at the top and bottom of the continent, respectively. Also shown on Figure 1 are eight selected example models labeled A, B, C, ... H, for future reference.

For the models that do lie in the range of eq. (1.3) for $\Omega_{\rm DM}h^2$, it is interesting to consider the searches for direct dark matter detection, with the most sensitive at this writing being the results from XENON100 in ref. [4], which superseded earlier results from CDMS [5]. In Figure 1, we show the ratio of the spin-independent LSP-nucleon cross section to the current XENON100 limit for that LSP mass, for model points in Figure 1 with $\Omega_{\rm DM}h^2 = 0.11$. The models are denoted by different symbols depending on what is the most important mechanism for dark matter annihilation in the early universe, and plotted both as a function of μ and of θ_{24}. However, it is important to realize that the models with $\sigma_{SI}/\sigma_{\rm XENON100} > 1$ are not ruled out, for several reasons. First, the would-be LSP may have decayed, either to a lighter singlet or by R-parity violation, or may have been diluted by late inflation. Second, there are significant uncertainties in the local density of dark matter, and especially in the nuclear matrix elements that go into the computation of σ_{SI}. These could easily reduce the true σ_{SI} by more than a factor of 2. Therefore, none of the models considered can be taken to be ruled out, but we see that within a default interpretation, most of the

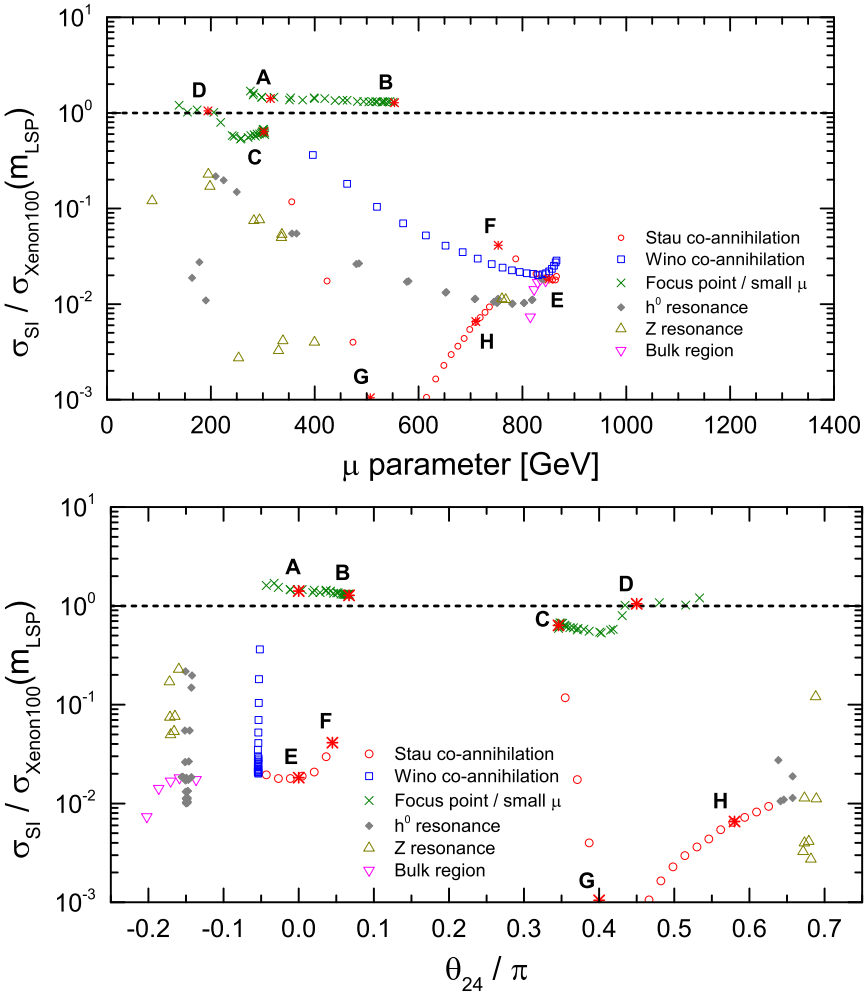

FIG. 2: The ratio of the spin-independent LSP-nucleon cross section to the current XENON100 limit for model points in Figure 1 (with fixed $M_3 = -A_0 = 600$ GeV, $\tan\beta = 10$, and $\mu > 0$ and varying θ_{24}, m_0) that have $\Omega_{\rm DM}h^2 = 0.11$. Different symbols are used for the model points according to which dark matter annihilation channels are most important in the early universe.

small-μ models in the CMSSM continent, and some of those within the right continent can be said to be challenged by the XENON100 results. In contrast, the stau co-annihilation, bulk region, and wino co-annihilation models are not at all challenged by the present direct dark matter searches in this model set. In the case of stau co-annihilation models with $\theta_{24}/\pi > 0.35$, σ_{SI} does not fall monotonically with μ, but instead falls sharply and by orders of magnitude where it is subject to accidental cancellations between the light and heavy Higgs contributions and other contributions. These cancellations are features of a leading order calculation, and including loop corrections and real emission diagrams should be expected to remove these accidental cancellations, but σ_{SI} can still be so small that direct detection will be quite problematic. The eight example model points

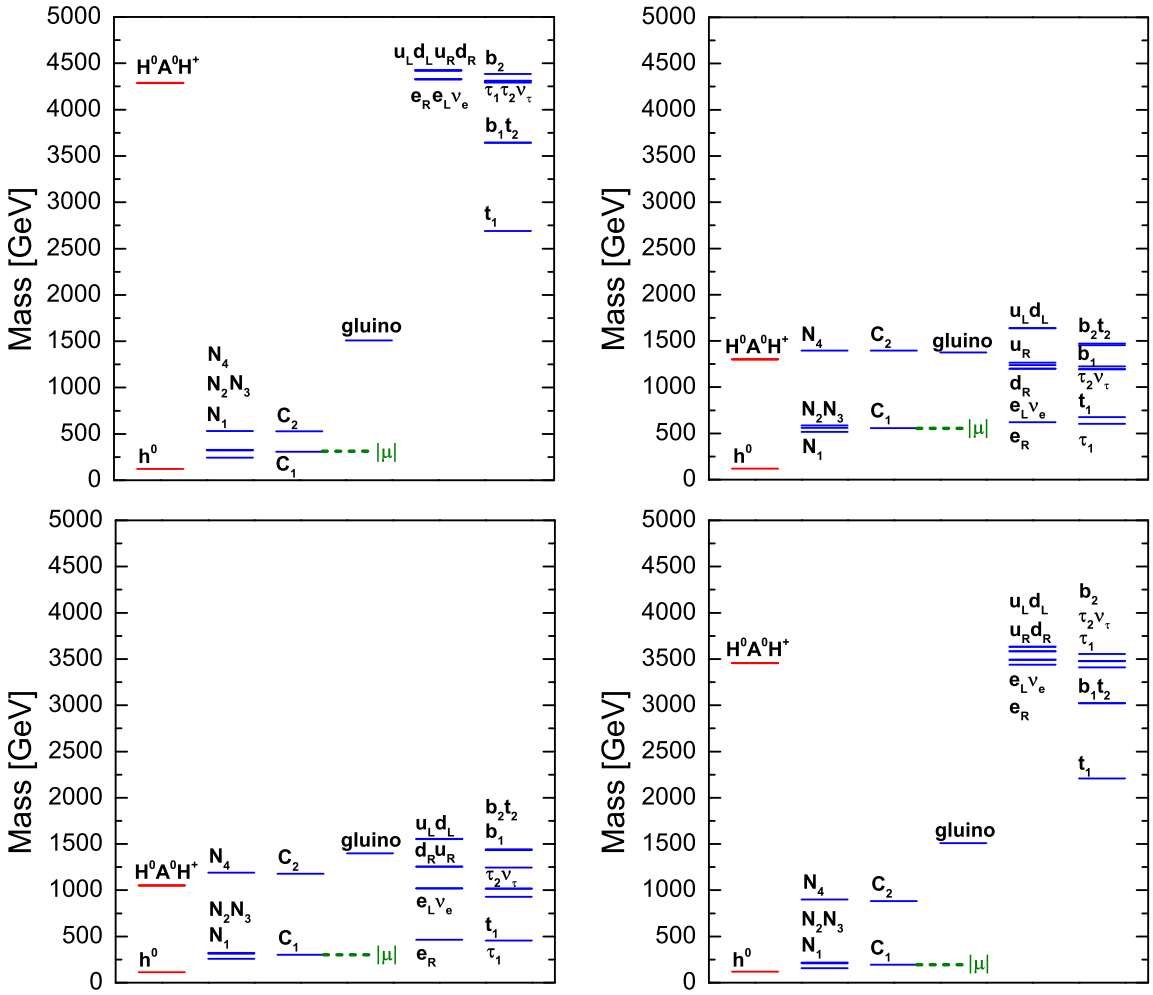

FIG. 3: Comparison of superpartner and Higgs mass spectra for four selected model points A,B,C,D (top left, top right, bottom left, and bottom right, respectively) in the small-μ dark matter regions in Figure 1.

from Figure 1 are labeled individually. Note that of the small-μ models, those with $\theta_{24}/\pi \lesssim 0.45$ most easily evade the dark matter direct detection searches.

As examples, we show in Figure 3 the superpartner and Higgs mass spectra for the four selected models with small μ and $\Omega_{\rm DM}h^2$ within the WMAP range, as labeled in Figures 1 and 2. The parameters for these models are $M_3 = -A_0 = 600$ GeV, $\tan\beta = 10$, and:

$$\text{A}: \quad (\theta_{24}/\pi,\ m_0) = (0.0,\ 4325\,\text{GeV}) \quad \text{focus point, central continent} \tag{3.2}$$

$$\text{B}: \quad (\theta_{24}/\pi,\ m_0) = (0.0671,\ 400\,\text{GeV}) \quad \text{small } \mu\text{, central continent} \tag{3.3}$$

$$\text{C}: \quad (\theta_{24}/\pi,\ m_0) = (0.346,\ 400\,\text{GeV}) \quad \text{small } \mu\text{, right continent} \tag{3.4}$$

$$\text{D}: \quad (\theta_{24}/\pi,\ m_0) = (0.45,\ 3440\,\text{GeV}) \quad \text{focus point, right continent} \tag{3.5}$$

Model A is a CMSSM focus point model, with the well-known features of squarks and sleptons

that are far too heavy to be seen at LHC, higgsino-like neutralinos and charginos that are lighter than their wino-like counterparts, and a Higgs boson that easily evades LEP bounds. Model D is qualitatively similar, although with a slightly lighter spectrum. This implies that in the case of model A, the final state of dark matter annihilation is mostly $t\bar{t}$, while it is mostly WW and ZZ in model D. In both of these models, discovery at the LHC will eventually come from gluino pair production to multi-jet final states.

In contrast, models B and C both have squarks that will be accessible to the LHC. Both models have significant hierarchies between the right-handed and left-handed sleptons, and between the right-handed and left-handed squarks. Eventual measurements of these masses would help to confirm the role played by large M_2/M_3 in these models. Both models also have small mass differences between the higgsino-like neutralino and chargino states $\tilde{N}_2, \tilde{N}_3, \tilde{C}_1$ and the LSP. In the case of model B, co-annihilations of all of these states are important in the early universe, while in model B the annihilation is mostly LSP pairs to $t\bar{t}$ and ZZ. We also note that the spin-independent nucleon-LSP cross-section is a factor of 4 smaller for model C than for model B, and the former is below the limit from XENON100 at that mass while the latter is above the limit, when computed using the default micrOMEGAs parameters. However, another key difference between these models is that the lightest Higgs mass m_h is in tension (near or possibly below) the LEP limit for model C, while it is about 119 GeV for model B.

We also show in Figure 4 the superpartner and Higgs mass spectra for the four selected models E,F,G,H with small m_0, leading to stau co-annihilation and slepton-mediated dark matter regions within the $\Omega_{\rm DM}h^2$ range from WMAP. The parameters for these models are $M_3 = -A_0 = 600$ GeV, $\tan\beta = 10$, and:

$$\text{E}: \quad (\theta_{24}/\pi,\, m_0) = (0.0,\, 140\,\text{GeV}) \quad \text{stau co-annihilation, central continent} \tag{3.6}$$

$$\text{F}: \quad (\theta_{24}/\pi,\, m_0) = (0.045,\, 215\,\text{GeV}) \quad \text{stau co-annihilation, central continent} \tag{3.7}$$

$$\text{G}: \quad (\theta_{24}/\pi,\, m_0) = (0.4,\, 125\,\text{GeV}) \quad \text{stau co-annihilation, right continent} \tag{3.8}$$

$$\text{H}: \quad (\theta_{24}/\pi,\, m_0) = (0.58,\, 68\,\text{GeV}) \quad \text{bulk (slepton-mediated), right continent} \tag{3.9}$$

Model E is a typical stau co-annihilation scenario within mSUGRA, with a small mass difference $m_{\tilde{\tau}_1} - m_{\tilde{N}_1} = 4.7$ GeV. It is beyond the reach of present LHC data, but will be eventually discovered in the jets+$E_T^{\rm miss}$ searches. The spin-independent nucleon-LSP cross-section is about a factor of 50 smaller than what would be necessary to probe this model with the published XENON100 searches. Model F is also a stau co-annihilation model, but with a much more compressed spectrum. In this model $m_{\tilde{\tau}_1} - m_{\tilde{N}_1}$ is less than 1 GeV. This small mass difference is needed in order for the co-

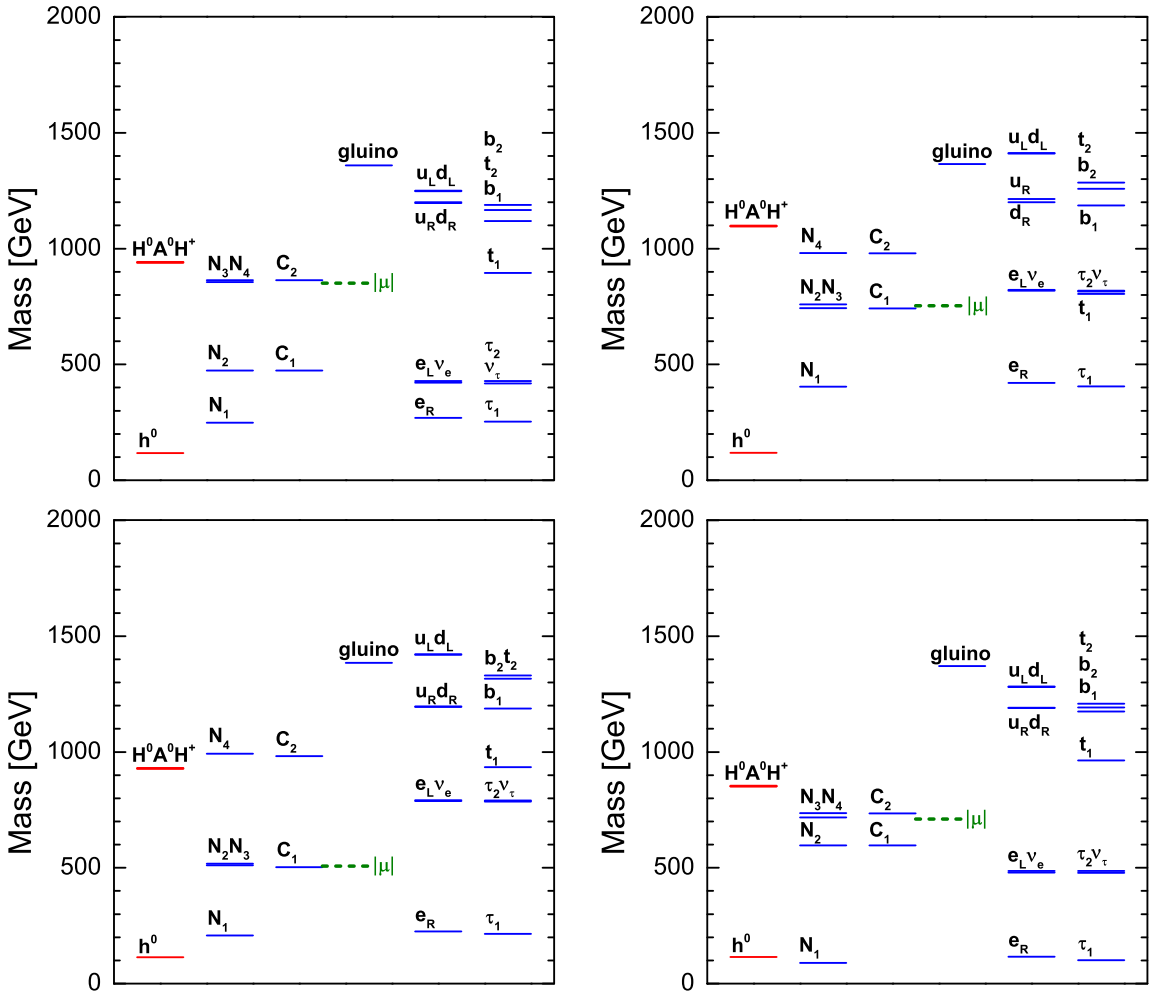

FIG. 4: Comparison of superpartner and Higgs mass spectra for four selected model points E,F,G,H (top left, top right, bottom left, and bottom right, respectively) in the stau co-annihilation and bulk (slepton-mediated) dark matter regions in Figure 1.

annihilations to be efficient, given the larger LSP mass, and it means that the lighter stau will have only four-body decays $\tilde{\tau}_1 \to \nu_\tau \overline{\nu}_\ell \ell \tilde{N}_1$ and will be stable on time scales relevant for colliders. However, direct production of stau pairs is very small, and staus occur only rarely in gluino and squark decays in this model, so the initial discover at LHC will again come from jets+$E_T^{\rm miss}$ searches. The spin-independent nucleon-LSP cross-section is only a factor of 8 below the present XENON100 limit for model F. Both models E and F have m_h well above the LEP limit.

Model G, in contrast, has σ_{SI} about three orders of magnitude below the XENON100 limit, so dark matter direct detection will probably be impossible in the foreseeable future. Otherwise, it is similar to the CMSSM model E, with the main qualitative differences being a Higgs mass that is closer to the LEP limit of 114 GeV and a somewhat larger mass difference $m_{\tilde{\tau}_1} - m_{\tilde{N}_1} = 7.0$

GeV. Model H is a bulk region model, with slepton-mediated annihilations $\tilde{N}_1\tilde{N}_1 \to e^+e^-$, $\mu^+\mu^-$, and $\tau^+\tau^-$ mostly responsible for dark matter annihilation in the early universe. The lightest stau is at $m_{\tilde{\tau}_1} = 102$ GeV, and about 13 GeV heavier than the LSP. Despite the low LSP mass, this model has σ_{SI} more than 2 orders of magnitude below the present XENON100 bounds. The LHC signatures of models G and H should be very similar to model E, and a careful measurement of the slepton-LSP mass differences will be crucial for inferring their dark matter properties.

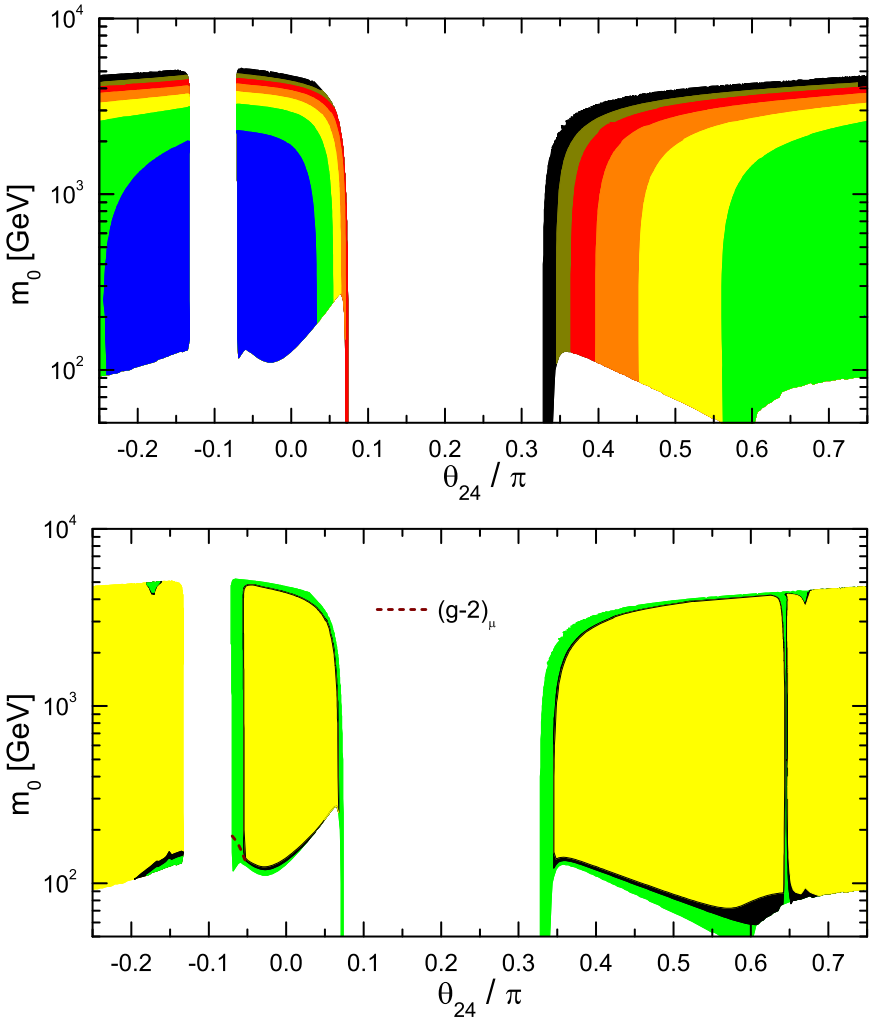

FIG. 5: Maps of the μ parameter (upper plot) and the predicted thermal relic abundance of dark matter $\Omega_{\rm DM}h^2$ (lower plot) in the θ_{24}, m_0 parameter space with fixed $M_3 = -A_0 = 600$ GeV, $\tan\beta = 10$, and $\mu < 0$. The correspondence of shaded regions to $|\mu|$ in the upper plot and to $\Omega_{\rm DM}h^2$ in the lower plot are the same as in Figure 1. The small corner near $\theta_{24}/\pi = -0.07$ and $m_0 = 150$ GeV is disfavored by the anomalous magnetic moment of the muon.

It is also interesting to consider the same slicing through parameter space but with $\mu < 0$. The map of $|\mu|$ and $\Omega_{\rm DM}h^2$ for this case is shown in Figure 5. The qualitative features for this case are very similar to the positive μ case. In a small corner of the allowed central continent for $m_0 < 200$ GeV and θ_{24}/π near -0.07, the anomalous magnetic moment of the muon constraint eliminates some models; the other indirect constraints from eqs. (2.4)-(2.8) do not play a role for these models. Note also that in Figure 5, the h^0 resonance region now is more pronounced on the right continent (rather than the left as for $\mu > 0$), providing solutions with $\Omega_{\rm DM}h^2 < 0.13$ near $\theta_{24}/\pi = 0.64$ that are continuously connected to the bulk region.

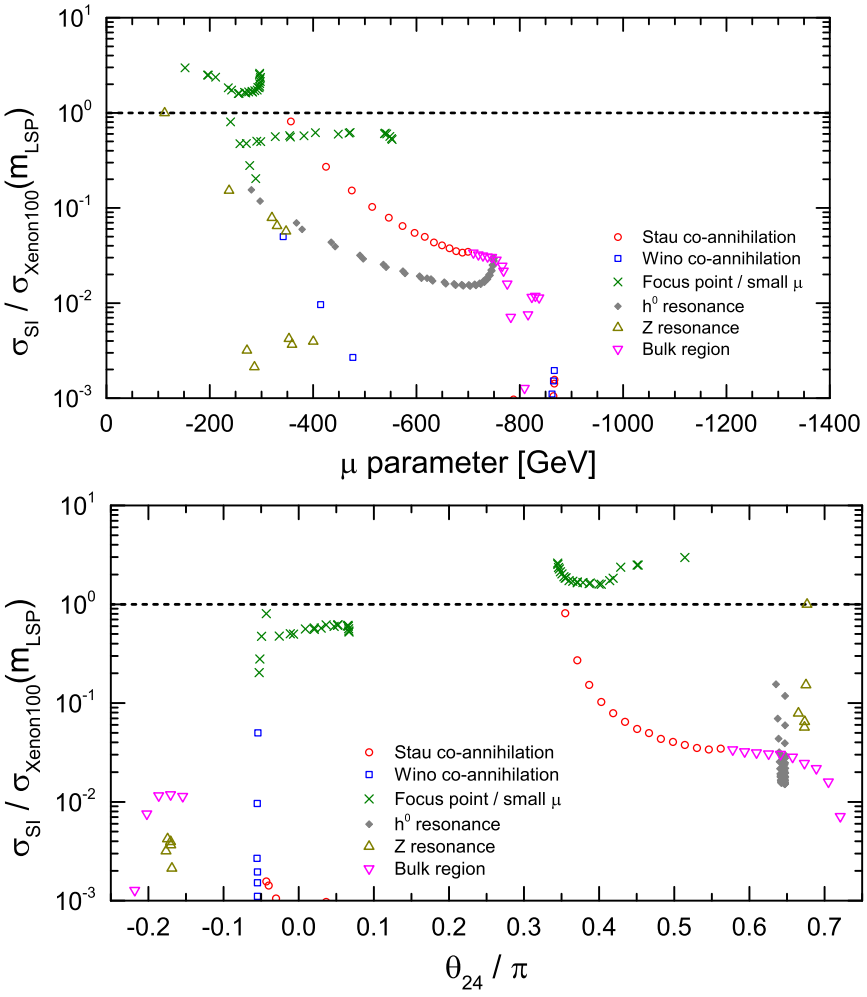

FIG. 6: The ratio of the spin-independent LSP-nucleon cross section to the current XENON100 limit for the model points in Figure 5 (with fixed $M_3 = -A_0 = 600$ GeV, $\tan\beta = 10$, and $\mu < 0$ and varying θ_{24}, m_0) that have $\Omega_{\rm DM}h^2 = 0.11$. Different symbols are used for the model points according to which dark matter annihilation channels are most important in the early universe.

Figure 1 shows the ratio of the spin-independent LSP-nucleon cross section to the current XENON100 limit for that LSP mass, for model points in Figure 1 with $\Omega_{\rm DM}h^2 = 0.11$. Here the most important feature that is different from the $\mu > 0$ case is that the small-$|\mu|$ models that are least susceptible to direct detection at XENON100 for $\mu < 0$ are those on the main, CMSSM-like continent. The focus point/small-μ models on the right, large-θ_{24} continent are nominally above the XENON100 limit, although we reiterate that this cannot be considered an exclusion.

We now consider the impact of large $\tan\beta$ on the allowed parameter space. To illustrate this, we consider in Figure 7 the allowed regions in the (θ_{24}, M_0) plane for $\tan\beta = 45$, with fixed $M_3 = -A_0 = 600$ GeV and $\mu > 0$. Here we note that the requirement of a neutralino LSP

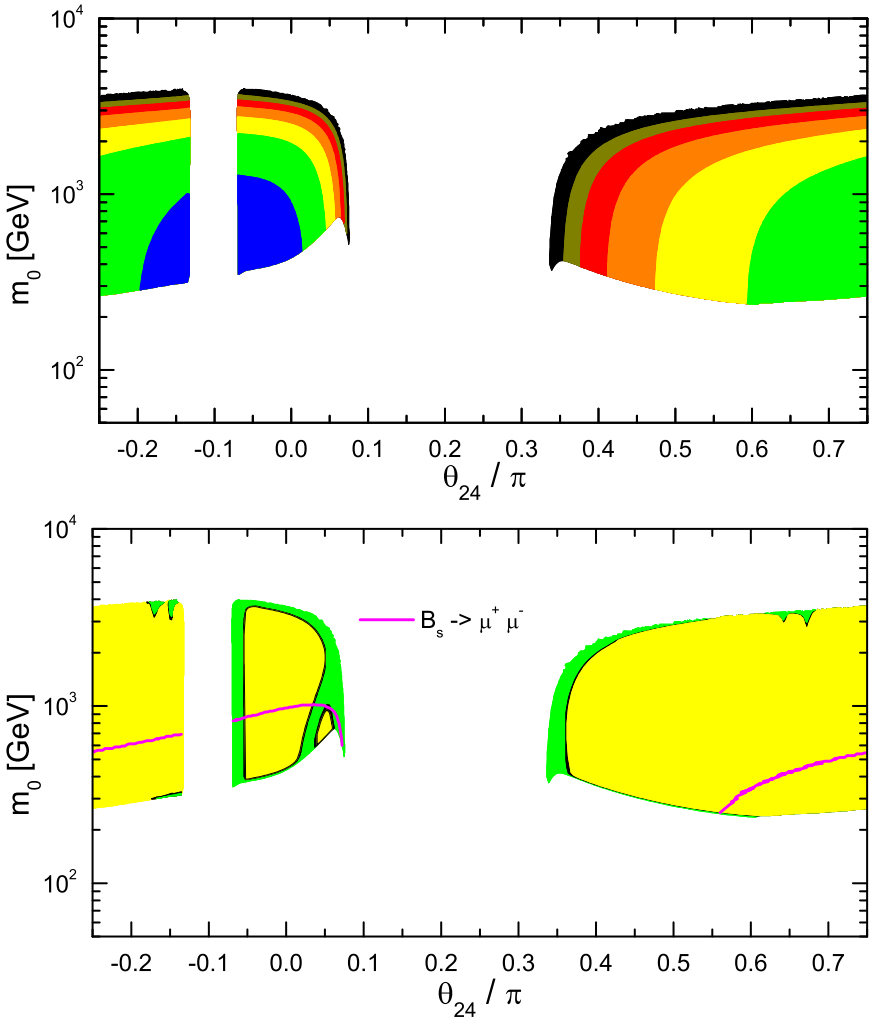

FIG. 7: Maps of the μ parameter (upper plot) and the predicted thermal relic abundance of dark matter $\Omega_{\rm DM}h^2$ (lower plot) in the θ_{24}, m_0 parameter space with fixed $M_3 = -A_0 = 600$ GeV, $\tan\beta = 45$, and $\mu > 0$. The correspondence of shaded regions to μ in the upper plot and to $\Omega_{\rm DM}h^2$ in the lower plot are the same as in Figures 1 and 5. The regions under the contour in the lower plot are disfavored by the limit on BR($B_s \to \mu^+\mu^-$).

constrains the scalar masses m_0 to be larger than the minimal values obtained for moderate $\tan\beta$. In the central continent of Figure 7, we note a channel of points with $\Omega_{\rm DM}h^2 < 0.09$; this is the A^0-resonance funnel, where dark matter annihilation is driven chiefly by s-channel pseudoscalar exchange, with $\Omega_{\rm DM}h^2 = 0.11 \pm 0.02$ regions on either side. This produces an island, centered near $\theta_{24}/\pi = 0.05$ and $m_0 = 700$ GeV and separate from the main CMSSM-connected continent, which is a confluence between the stau co-annihilation, low-μ, and A^0 funnel mechanisms for efficient dark matter annihilation. However, this island is disfavored at 95% level by the constraint from BR($B_s \to \mu^+\mu^-$) $< 1.1 \times 10^{-8}$. More generally, this constraint eliminates all of the stau co-

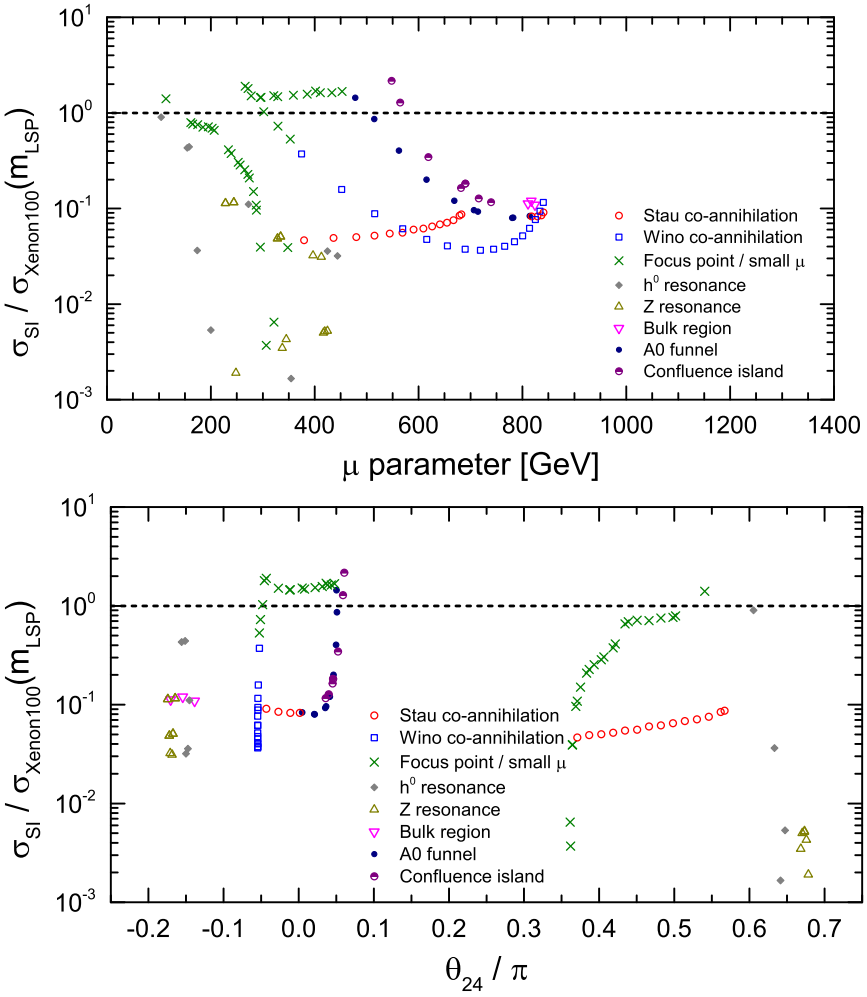

FIG. 8: The ratio of the spin-independent LSP-nucleon cross section to the current XENON100 limit for the model points in Figure 7 (with fixed $M_3 = -A_0 = 600$ GeV, $\tan\beta = 45$, and $\mu > 0$ and varying θ_{24}, m_0) that have $\Omega_{\rm DM}h^2 = 0.11$. Different symbols are used for the model points according to which dark matter annihilation channels are most important in the early universe.

annihilation and bulk region models on the central and left continents. On the right continent, however, a large number of stau co-annihilation models on the small-m_0 edge do survive, with values of μ ranging up to 700 GeV. The top edges of the central and right continents are small-μ regions, as before, while on the left edge of the right continent, near $\theta_{24}/\pi = 0.36$, both s-channel A^0 exchange and a significant higgsino content of the LSP play a role in dark matter annihilation.

The ratio $\sigma_{SI}/\sigma_{\rm XENON100}$ for these models with $\tan\beta = 45$ are shown in Figure 8. Again we note that models with small $\mu > 0$ are most challenged by the XENON100 limits on the central, CMSSM-like continent. The models on the left side of the right continent, where the pseudoscalar exchange assists the higgsino content of the LSP in dark matter annihilations, tend to be far

below the nominal XENON100 bounds even with the standard interpretation of those limits. As before, models with wino co-annihilation, A^0 resonance, h^0 resonance, and Z resonance as the dark matter annihilation mechanisms tend to be unchallenged by present direct detection limits as well. Although we did not encounter models in which the correct relic abundance of dark matter is brought about by stop or sbottom co-annihilations [42, 43], there is no general reason why they should not exist, in particular if the assumption of a common scalar squared mass m_0^2 were relaxed.

IV. EXPLORATIONS WITH FIXED M_1

In this section, we consider alternative slices in parameter space with M_1 held fixed. This implies that in most of the parameter space, the LSP has a mass that does not vary greatly within the graphs to be presented below. With fixed M_1, the parameterization of eqs. (2.1)-(2.3) can be written as

$$M_2 \;=\; M_1 \left(\frac{1+3\tan\theta_{24}}{1+\tan\theta_{24}}\right), \qquad M_3 \;=\; M_1 \left(\frac{1-2\tan\theta_{24}}{1+\tan\theta_{24}}\right). \tag{4.1}$$

Therefore, fixing M_1 implies that M_2 and M_3 become very large when θ_{24}/π approaches $-1/4$ and $3/4$, so we again choose those asymptote values as the boundaries of the range, and again the parameter space splits into three main continents. At $\theta_{24}/\pi \approx -0.102$, one has M_2 approaching 0, so models near this vertical line are excluded, providing an ocean between the two continents. Similarly, at $\theta_{24}/\pi \approx 0.148$, one has M_3 approaching 0, so models near this vertical line are likewise excluded, providing another gap between the two continents of viable parameter space on either side. The boundaries of the continents on either side of the $M_3 = 0$ line are actually determined by the fact that small $|M_3/M_2|$ leads to small $|\mu|^2$, as can be seen from eqs. (1.1) and (1.2).

We consider first models with fixed $M_1 = -A_0 = 500$ GeV, $\tan\beta = 10$, and $\mu > 0$. The maps of μ and $\Omega_{\rm DM}h^2$ for these models are shown in Figure 9. The allowed regions are qualitatively similar to the case discussed above for Figure 1, except that in this case there is a region in which light top squarks mediate the dark matter annihilation, for $0.055 \lesssim \theta_{24}/\pi \lesssim 0.08$ and 100 GeV $\lesssim m_0 \lesssim 600$ GeV, as in ref. [30]. This region is now likely to be ruled out[†] by LHC searches because the gluino is lighter than 660 GeV here, and the average squark mass is not much higher, although there is no experimental search specifically sensitive to this particular version of compressed supersymmetry. More generally, the regions of the plane that the current LHC published searches are sensitive to are roughly indicated by the $m_{\tilde q} = 800$, 1000 GeV contours shown in the lower plot of Figure 9. Other regions have heavier squarks and/or gluinos. Note in particular that the left side of the right continent has gluino masses above 1.1 TeV, and increasing as one moves to the right. The region from $0.11 \lesssim \theta_{24}/\pi \lesssim 0.33$ where one might have expected to find lighter gluinos was already excluded because $-m^2_{H_u}$ is negative at the TeV scale, precluding electroweak symmetry breaking.

[†] However, similar models with non-universal scalar masses, in particular with larger gluino and first- and second-family squark masses, could evade these LHC searches. The LHC signatures for this scenario would include, besides the usual jets plus $E_T^{\rm miss}$ events, events with same-sign top quarks [44] and eventually striking resonant diphoton decays of stoponium [45, 46], a bound state of top squarks. Stoponium is long-lived enough to form bound states in these models because of the absence of two-body flavor-preserving decays of the top squark.

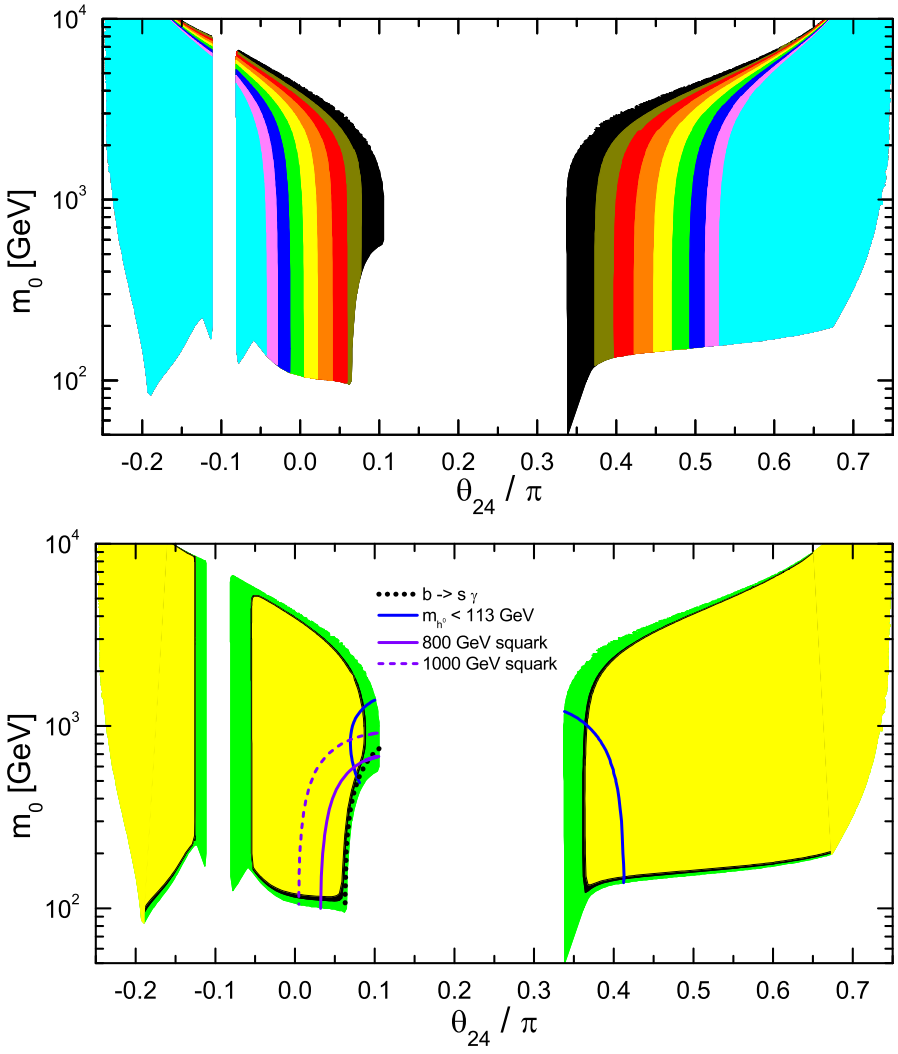

FIG. 9: Maps of the μ parameter (upper plot) and the predicted thermal relic abundance of dark matter $\Omega_{\rm DM}h^2$ (lower plot) in the θ_{24}, m_0 parameter space with fixed $M_1 = -A_0 = 500$ GeV, $\tan\beta = 10$, and $\mu > 0$. In the upper plot, the dark (black) regions closest to the center represent $\mu < 300$ GeV, and successive regions away from the center correspond to 300 GeV $< \mu <$ 400 GeV (brown) and 400 GeV $< \mu <$ 500 GeV (red) and so on up to the last region (cyan) which corresponds to $\mu > 1000$ GeV. Regions left blank do not have viable electroweak symmetry breaking, do not have a neutralino as the LSP, or have superpartners that are too light, as described in the text. In the lower plot, the thin dark regions (black) correspond to the observed range $0.09 < \Omega_{\rm DM}h^2 < 0.13$. The large interior regions (yellow) correspond to $\Omega_{\rm DM}h^2 > 0.13$, while the darker shaded exterior region (green) has $\Omega_{\rm DM}h^2 < 0.09$. Also indicated are contours for $m_{h^0} < 113$ GeV, for BR$(b \to s\gamma)$ from eq. (2.7), and for $m_{\tilde{q}} = 800, 1000$ GeV corresponding roughly to the present LHC data reach, with regions closer to the center disfavored in each case.

Because the gluino mass increases as one moves away from the center of the plots, μ also increases, and unlike the fixed-M_3 plots of the previous section, there are now models with μ well above 1 TeV. This illustrates the fine-tuning price of moving to gluino and squark masses far above the LHC-accessible regions.

Also indicated in Figure 9 are regions that are disfavored by the BR($b \to s\gamma$) and m_h limits. Recall, however, that the first of these can be evaded by intrinsically supersymmetry-breaking flavor violation. Moreover, it is now weaker than the probable direct reach of LHC in this particular parameter space slice. Note that these constraints eliminate the stau co-annihilation region with smaller μ on the CMSSM continent, but leave regions with $\mu > 450$ GeV on the right continent. The focus-point/small-μ regions on the top edges of the continents are untouched by these constraints, and we note that, as before, moving from the CMSSM focus point case to $\theta_{24} > 0$ reduces the values of m_0 required for small μ and favorable dark matter, thus arguably substantially decreasing the fine-tuning cost. However, in the fixed $M_1 = 500$ GeV parameter space, the m_h constraint still imposes the requirement that m_0 is well above 1 TeV. Taking larger M_1 would ameliorate this, as should be clear from the fixed $M_3 = 600$ GeV cases studied above.

Figure 10 shows the ratio of the spin-independent LSP-nucleon cross section to the current XENON100 limit for the model points in Figure 9. For fixed M_1, we see the well-known fact that the correlation between the higgsino content of the LSP, inversely proportional to $|\mu/M_1|$ for these models, and the spin-independent cross-section is quite robust, with models having $\mu < 110$ GeV strongly challenged within the standard interpretation of the LSP as dark matter (but not ruled out, as noted above). This includes especially the small-μ models with smaller m_0 (i.e., the models near $\theta_{24}/\pi = 0.07$ and 0.37. Conversely, stau co-annihilation and wino co-annihilation models not otherwise ruled out are fine, and models with $\mu > 300$ are two orders of magnitude away from the sensitivity in direct dark matter experiments needed to challenge them, within this slice of parameter space.

As a final exploration, we consider models with fixed $M_1 = -A_0 = 900$ GeV and $\tan\beta = 45$, with $\mu > 0$. The maps of μ and $\Omega_{\rm DM}h^2$ are shown in Figure 11 as before. Notable features include the facts that regions with small μ are much thinner within this parameter space, and there are no viable regions with m_0 less than about 500 GeV. As in the case of fixed M_3 with large $\tan\beta$ in the previous section, there is a confluence island, on the shores of which A^0 resonance, stau co-annihilation, and small-μ play a role in reducing the dark matter density. However, again the $B_s \to \mu^+\mu^-$ constraint strongly disfavors this island, and the smaller μ part of it is also disfavored by $B \to \tau\nu$ and $b \to s\gamma$. On the right continent, there is another large island nearly split off from

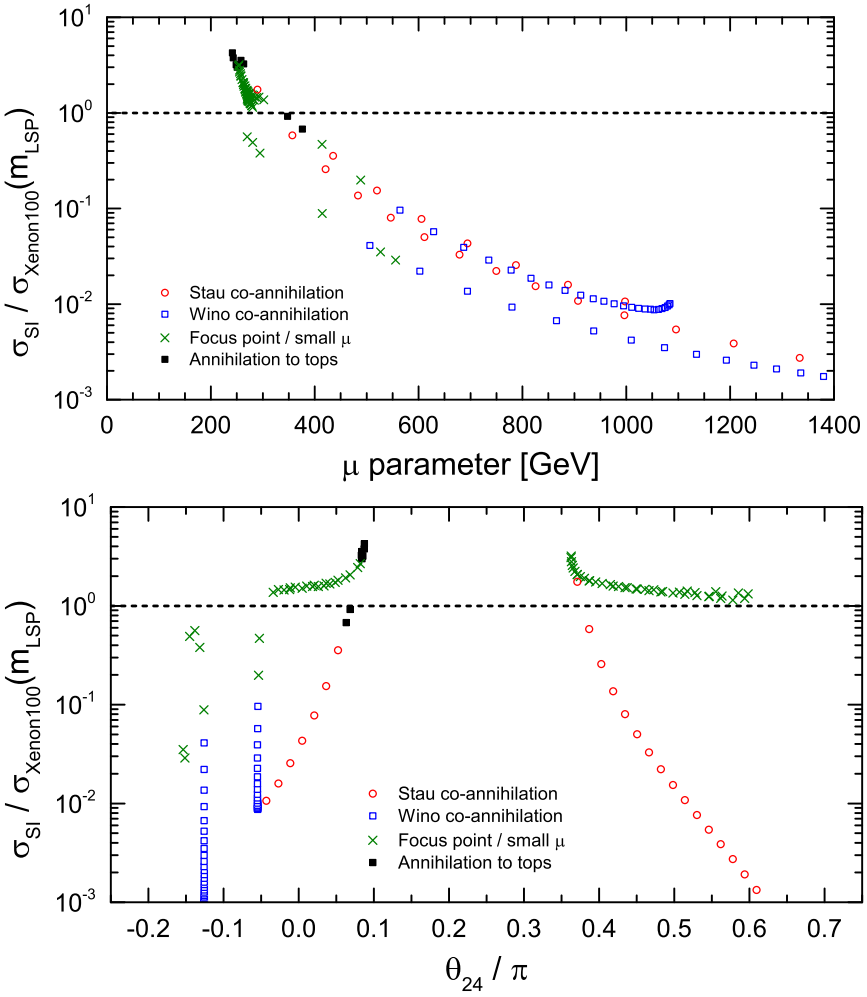

FIG. 10: The ratio of the spin-independent LSP-nucleon cross section to the current XENON100 limit for the model points in Figure 9 (with fixed $M_1 = -A_0 = 500$ GeV, $\tan\beta = 10$, and $\mu > 0$ and varying θ_{24}, m_0) that have $\Omega_{\rm DM}h^2 = 0.11$. Different symbols are used for the model points according to which dark matter annihilation channels are most important in the early universe.

the main continent by a channel consisting of an A^0 resonance funnel region. On the top edge of this island, pseudoscalar exchange plays the main role in the annihilation of dark matter, while on the lower edge it is mainly stau co-annihilation. The entire $\Omega_{\rm DM}h^2 < 0.13$ part of this continent is free from the indirect constraints eq. (2.4)-(2.8). It is also not challenged by dark matter direct detection, except perhaps for the top edge with small μ, as can be seen in Figure 12. This is more generally true of all models within this slice of parameter space with $\mu > 180$ GeV.

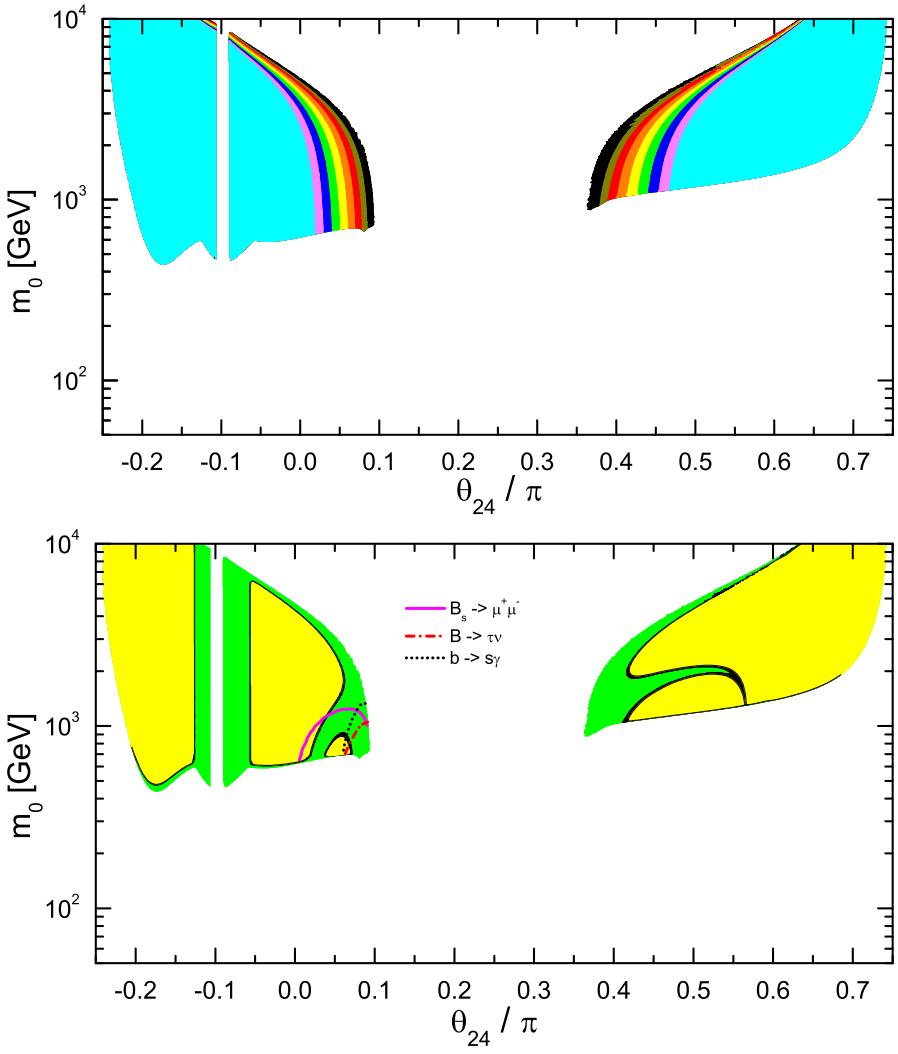

FIG. 11: Maps of the μ parameter (upper plot) and the predicted thermal relic abundance of dark matter $\Omega_{\rm DM}h^2$ (lower plot) in the θ_{24}, m_0 parameter space with fixed $M_1 = -A_0 = 900$ GeV, $\tan\beta = 45$, and $\mu > 0$. The correspondence of shaded regions to μ values in the upper plot and to $\Omega_{\rm DM}h^2$ in the lower plot are the same as in Figure 9. Also indicated are contours as described in the text for the branching ratios of $B_s \to \mu^+\mu^-$ and $B \to \tau\nu$ and $b \to s\gamma$.

V. OUTLOOK

As LHC searches continue to push the bounds on superpartner masses higher, there appears to be growing tension between the weak scale m_Z and the dimensionful supersymmetry-breaking terms that determine it from the effective potential. Non-universal gaugino masses provide a way of ameliorating this fine-tuning issue. In this paper we showed that there are large regions of parameter space in which $|\mu|$ as determined by the supersymmetry-breaking Lagrangian is naturally

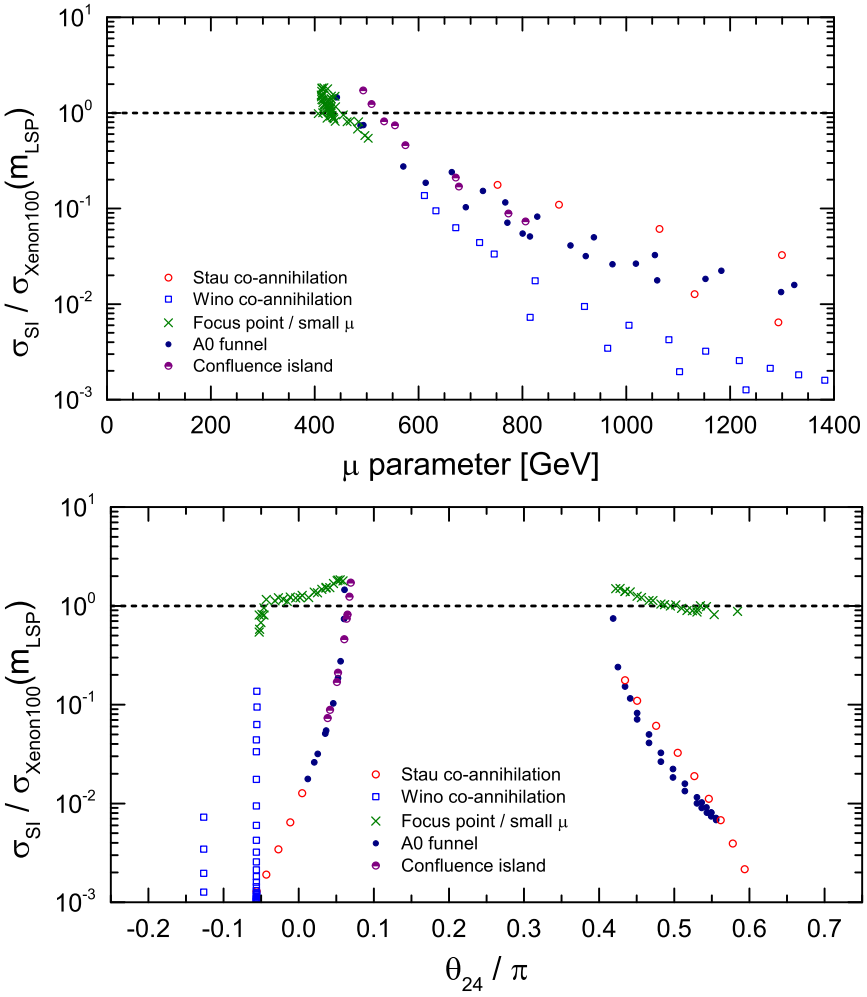

FIG. 12: The ratio of the spin-independent LSP-nucleon cross section to the current XENON100 limit for the model points in Figure 11 (with fixed $M_1 = -A_0 = 900$ GeV, $\tan\beta = 45$, $\mu > 0$ and varying θ_{24}, m_0) that have $\Omega_{\rm DM}h^2 = 0.11$. Different symbols are used for the model points according to which dark matter annihilation channels are most important in the early universe.

small, while scalar masses can be much less than the several TeV scale found in the traditional focus-point region in the MSSM. These models do evade the present bounds set by the LHC, but are now being confronted by dark matter direct detection experiments. However, exclusion is not possible with present XENON100 bounds for most of the cases we looked at, even if R-parity is conserved and the lightest neutralino is really the dark matter. As is well-known, since the spin-independent cross section increases with higgsino content of the LSP, which in turn increases as $|\mu|$ decreases, future dark matter direct detection searches will probe the more natural models first.

In this paper, we also showed how non-universal gaugino masses can provide for a bulk region in which t-channel slepton exchange (without significant co-annihilations) plays the dominant role

in annihilating the dark matter down to acceptable levels in the early universe. This is interesting because this region is severely endangered or perhaps extinct within the CMSSM after LHC and LEP bounds are considered. We further mapped out the regions in which stau co-annihilations and Higgs resonance play the most important role in dark matter annihilations; these regions differ in interesting ways from the corresponding CMSSM scenarios, and are not always continuously connected to them. In order to keep our study finite, we did not consider scalar mass non-universality here, but other works (see for example [22] and references therein) have showed that non-universal Higgs mass models have large variations in the dark matter relic density and spin-independent cross-sections. If supersymmetry is discovered at the LHC and in direct dark matter detection experiments, it will be a challenge to understand to what extent non-universalities in the soft supersymmetry breaking parameters play a role in determining the phenomenological collider and dark matter properties of the theory.

As this paper was being prepared, the ATLAS and CMS detector collaborations announced hints [47] of a Higgs scalar boson signal in the vicinity of $M_h = 125$ GeV. If these hints are confirmed, the impact on the models considered here would be profound, as most of the parameter space cannot accommodate such large M_h values. If one assigns a combined 3 GeV uncertainty (note that this is a somewhat arbitrary estimate, including both the theoretical uncertainty of about 2 GeV [48] and the quite preliminary LHC uncertainty) to M_h, and therefore considers regions with predicted $M_h \gtrsim 122$ GeV to be acceptable, then among the models we considered only those with moderately negative θ_{24} (on the main continent) and large m_0 are viable. From the point of view of the putative $M_h = 125$ GeV signal, the variation on the usual CMSSM focus point region with negative θ_{24} is therefore preferred. There are several other ways to increase the prediction for M_h, including by raising all of the soft masses (by raising M_3 in our framework) and by increasing $\tan\beta$. However, among the models considered here, the heavy scalar solutions with negative θ_{24} would seem to be the easiest to make consistent with $M_h \approx 125$ GeV. Other mechanisms, such as adding new vector-like supermultiplets [49]-[53], would affect our results in qualitative ways.

Acknowledgments: This work was supported in part by the National Science Foundation grant numbers PHY-0757325 and PHY-1068369. The work of JEY was supported in part by the U.S. National Science Foundation, grant NSF-PHY-0705682, the LHC Theory Initiative, Jonathan Bag-

ger, PI.

---

[1] S.P. Martin, "A supersymmetry primer," [hep-ph/9709356] (version 6, September 2011). M. Drees, R. Godbole and P. Roy, "Theory and phenomenology of sparticles: An account of four-dimensional N=1 supersymmetry in high energy physics," *World Scientific (2004)*. H. Baer and X. Tata, "Weak scale supersymmetry: From superfields to scattering events," *Cambridge University Press (2006)*. The first reference uses the same conventions employed here.

[2] G. Aad *et al.* [ATLAS Collaboration], "Search for squarks and gluinos using final states with jets and missing transverse momentum with the ATLAS detector in sqrt(s) = 7 TeV proton-proton collisions," arXiv:1109.6572 [hep-ex], "Search for new phenomena in final states with large jet multiplicities and missing transverse momentum using sqrt(s)=7 TeV pp collisions with the ATLAS detector," arXiv:1110.2299 [hep-ex], "Search for supersymmetry in final states with jets, missing transverse momentum and one isolated lepton in sqrts = 7 TeV pp collisions using 1 fb^{-1} of ATLAS data," arXiv:1109.6606 [hep-ex], "Search for supersymmetry in pp collisions at sqrt(s) = 7 TeV in final states with missing transverse momentum, b-jets and one lepton with the ATLAS detector" ATLAS-CONF-2011-130, "Search for supersymmetry in pp collisions at sqrt(s) = 7 TeV in final states with missing transverse momentum, b-jets and no leptons with the ATLAS detector", ATLAS-CONF-2011-098. New results can be found at:
`https://twiki.cern.ch/twiki/bin/view/AtlasPublic/SupersymmetryPublicResults`

[3] S. Chatrchyan *et al.* [CMS Collaboration], "Search for Supersymmetry at the LHC in Events with Jets and Missing Transverse Energy," arXiv:1109.2352 [hep-ex], "Search for supersymmetry in all-hadronic events with missing energy", CMS-PAS-SUS-11-004, "Search for supersymmetry in all-hadronic events with MT2", CMS-PAS-SUS-11-005, "Search for new physics with same-sign isolated dilepton events with jets and missing energy", CMS-PAS-SUS-11-010; "Search for new physics in events with opposite-sign dileptons and missing transverse energy", CMS-PAS-SUS-11-011; "Searches for Supersymmetry using Multilepton Signatures in pp Collisions at 7 TeV", CMS-PAS-SUS-11-013; "Search for supersymmetry in events with a lepton and missing energy" CMS-PAS-SUS-11-015, "Search for New Physics in Events with b-quark Jets and Missing Transverse Energy in Proton-Proton Collisions at 7 TeV", CMS-PAS-SUS-11-006. New results can be found at:
`https://twiki.cern.ch/twiki/bin/view/CMSPublic/PhysicsResultsSUS`

[4] E. Aprile *et al.* [XENON100 Collaboration], Phys. Rev. Lett. **107**, 131302 (2011) [arXiv:1104.2549 [astro-ph.CO]].

[5] Z. Ahmed *et al.* [The CDMS-II Collaboration], Science **327**, 1619 (2010) [0912.3592 [astro-ph.CO]].

[6] S. Schael *et al.* [ALEPH and DELPHI and L3 and OPAL and LEP Working Group for Higgs Boson Searches Collaborations], Eur. Phys. J. **C47**, 547-587 (2006). [hep-ex/0602042].

[7] S.P. Martin and M.T. Vaughn, Phys. Rev. D **50**, 2282 (1994) [hep-ph/9311340]; Y. Yamada, Phys. Rev. D **50**, 3537 (1994) [hep-ph/9401241]; I. Jack and D.R.T. Jones, Phys. Lett. B **333**, 372 (1994) [hep-ph/9405233]; I. Jack, D.R.T. Jones, S.P. Martin, M.T. Vaughn and Y. Yamada, Phys. Rev. D **50**, 5481 (1994) [hep-ph/9407291].

[8] G.L. Kane and S.F. King, Phys. Lett. B **451**, 113 (1999) [hep-ph/9810374], M. Bastero-Gil, G.L. Kane and S.F. King, Phys. Lett. B **474**, 103 (2000) [hep-ph/9910506].

[9] J.R. Ellis, C. Kounnas and D.V. Nanopoulos, Nucl. Phys. B **247**, 373 (1984), J.R. Ellis, K. Enqvist, D.V. Nanopoulos and K. Tamvakis, Phys. Lett. B **155**, 381 (1985), M. Drees, Phys. Lett. B **158**, 409 (1985), G. Anderson, C.H. Chen, J.F. Gunion, J.D. Lykken, T. Moroi and Y. Yamada, "Motivations for and implications of non-universal GUT-scale boundary conditions for soft SUSY-breaking parameters," *In the Proceedings of 1996 DPF / DPB Summer Study on New Directions for High-Energy Physics (Snowmass 96)*, [hep-ph/9609457]. G. Anderson, H. Baer, C.h. Chen and X. Tata, Phys. Rev. D **61**, 095005 (2000) [hep-ph/9903370].

[10] J. Chakrabortty and A. Raychaudhuri, Phys. Lett. B **673**, 57 (2009) [hep-ph/0812.2783], S.P. Martin, Phys. Rev. D **79**, 095019 (2009) [hep-ph/0903.3568].

[11] J.R. Ellis, T. Falk and K.A. Olive, Phys. Lett. B **444**, 367 (1998) [hep-ph/9810360]; J.R. Ellis, T. Falk, K.A. Olive and M. Srednicki, Astropart. Phys. **13**, 181 (2000) [Erratum-ibid. **15**, 413 (2001)] [hep-ph/9905481].

[12] J.L. Feng, K.T. Matchev and F. Wilczek, Phys. Lett. B **482**, 388 (2000) [hep-ph/0004043]. The focus point region is motivated by properties of the renormalization group equations that allow small μ, see: K.L. Chan, U. Chattopadhyay and P. Nath, Phys. Rev. D **58**, 096004 (1998) [hep-ph/9710473], J.L. Feng, K.T. Matchev and T. Moroi, Phys. Rev. Lett. **84**, 2322 (2000) [hep-ph/9908309]; Phys. Rev. D **61**, 075005 (2000) [hep-ph/9909334].

[13] M. Drees and M.M. Nojiri, Phys. Rev. D **47**, 376 (1993) [hep-ph/9207234].

[14] A. Birkedal-Hansen and B.D. Nelson, Phys. Rev. D **64**, 015008 (2001) [hep-ph/0102075].

[15] G.B. Gelmini and P. Gondolo, Phys. Rev. D **74**, 023510 (2006) [arXiv:hep-ph/0602230]. G.B. Gelmini, P. Gondolo, A. Soldatenko and C.E. Yaguna, Phys. Rev. D **74**, 083514 (2006) [arXiv:hep-ph/0605016].

[16] E. Komatsu *et al.* [WMAP Collaboration], Astrophys. J. Suppl. **192**, 18 (2011) [arXiv:1001.4538 [astro-ph.CO]]. D.N. Spergel *et al.* [WMAP Collaboration], Astrophys. J. Suppl. **148**, 175 (2003) [astro-ph/0302209], and [astro-ph/0603449]. M. Tegmark *et al.* [SDSS Collaboration], Phys. Rev. D **69**, 103501 (2004) [astro-ph/0310723];

[17] S.F. King, J.P. Roberts and D. P. Roy, JHEP **0710**, 106 (2007) [arXiv:0705.4219 [hep-ph]].

[18] H. Baer, A. Mustafayev, H. Summy and X. Tata, JHEP **0710**, 088 (2007) [arXiv:0708.4003 [hep-ph]].

[19] K. Huitu, R. Kinnunen, J. Laamanen, S. Lehti, S. Roy and T. Salminen, Eur. Phys. J. C **58**, 591 (2008) [arXiv:0808.3094 [hep-ph]].

[20] U. Chattopadhyay, D. Das and D. P. Roy, Phys. Rev. D **79**, 095013 (2009) [arXiv:0902.4568 [hep-ph]].

[21] S. Bhattacharya and J. Chakrabortty, Phys. Rev. D **81**, 015007 (2010) [arXiv:0903.4196 [hep-ph]].

[22] J. Ellis, K.A. Olive and P. Sandick, New J. Phys. **11**, 105015 (2009) [arXiv:0905.0107 [hep-ph]].

[23] I. Gogoladze, M.U. Rehman and Q. Shafi, Phys. Rev. D **80**, 105002 (2009) [arXiv:0907.0728 [hep-ph]], I. Gogoladze, R. Khalid and Q. Shafi, Phys. Rev. D **80**, 095016 (2009) [arXiv:0908.0731 [hep-ph]].

[24] D. Horton and G. G. Ross, Nucl. Phys. B **830**, 221 (2010) [arXiv:0908.0857 [hep-ph]].

[25] T. Li, J. A. Maxin and D. V. Nanopoulos, Phys. Lett. B **701**, 321 (2011) [arXiv:1002.1031 [hep-ph]], T. Li and D. V. Nanopoulos, Phys. Lett. B **692**, 121 (2010) [arXiv:1002.4183 [hep-ph]].

[26] N. Chen, D. Feldman, Z. Liu, P. Nath and G. Peim, Phys. Rev. D **83**, 035005 (2011) [arXiv:1011.1246 [hep-ph]].

[27] N. Okada, S. Raza and Q. Shafi, Phys. Rev. D **84**, 095018 (2011) [arXiv:1107.0941 [hep-ph]].

[28] M. Guchait, D. P. Roy and D. Sengupta, Phys. Rev. D **85**, 035024 (2012) [arXiv:1109.6529 [hep-ph]].

[29] I. Gogoladze, Q. Shafi and C. S. Un, arXiv:1112.2206 [hep-ph].

[30] S.P. Martin, Phys. Rev. D **75**, 115005 (2007) [hep-ph/0703097], Phys. Rev. D **76**, 095005 (2007) [hep-ph/0707.2812],

[31] B.C. Allanach, "SOFTSUSY: A C++ program for calculating supersymmetric spectra," Comput. Phys. Commun. **143**, 305 (2002) [hep-ph/0104145].

[32] A. Djouadi, J.L. Kneur and G. Moultaka, Comput. Phys. Commun. **176**, 426 (2007) [arXiv:hep-ph/0211331].

[33] G. Belanger, F. Boudjema, A. Pukhov and A. Semenov, Comput. Phys. Commun. **180**, 747 (2009) [hep-ph/0803.2360], Comput. Phys. Commun. **176**, 367 (2007) [hep-ph/0607059], Comput. Phys. Commun. **174**, 577 (2006) [hep-ph/0405253], Comput. Phys. Commun. **149**, 103 (2002) [hep-ph/0112278].

[34] M. Bona *et al.* [UTfit Collaboration], Phys. Lett. B **687**, 61 (2010) [arXiv:0908.3470 [hep-ph]].

[35] S. Chatrchyan *et al.* [CMS Collaboration], arXiv:1107.5834 [hep-ex].

[36] G.W. Bennett *et al.* [Muon G-2 Collaboration], Phys. Rev. D **73**, 072003 (2006) [arXiv:hep-ex/0602035], Phys. Rev. Lett. **92**, 161802 (2004) [arXiv:hep-ex/0401008], Phys. Rev. Lett. **89**, 101804 (2002) [Erratum-ibid. **89**, 129903 (2002)] [arXiv:hep-ex/0208001].

[37] S.P. Martin and J. D. Wells, Phys. Rev. D **67**, 015002 (2003) [arXiv:hep-ph/0209309].

[38] K. Nakamura *et al.* [Particle Data Group Collaboration], J. Phys. G **G37**, 075021 (2010).

[39] T.J. LeCompte and S.P. Martin, Phys. Rev. D **84**, 015004 (2011) [arXiv:1105.4304 [hep-ph]], Phys. Rev. D **85**, 035023 (2012) [arXiv:1111.6897 [hep-ph]].

[40] S.P. Martin and M.T. Vaughn, Phys. Lett. B **318**, 331 (1993) [hep-ph/9308222]. Y. Yamada, Phys. Lett. B **623**, 104 (2005) [hep-ph/0506262]. S.P. Martin, Phys. Rev. D **72**, 096008 (2005) [hep-ph/0509115], Phys. Rev. D **74**, 075009 (2006) [hep-ph/0608026].

[41] P. Nath and R. Arnowitt, Phys. Rev. Lett. **70**, 3696 (1993) [hep-ph/9302318]; A. Djouadi, M. Drees and J.L. Kneur, Phys. Lett. B **624**, 60 (2005) [hep-ph/0504090].

[42] M.E. Gomez, G. Lazarides and C. Pallis, Phys. Rev. D **61**, 123512 (2000) [hep-ph/9907261]; C. Boehm, A. Djouadi and M. Drees, Phys. Rev. D **62**, 035012 (2000) [hep-ph/9911496]; J.R. Ellis, K.A. Olive and Y. Santoso, Astropart. Phys. **18**, 395 (2003) [hep-ph/0112113]; C. Balazs, M. Carena and C.E.M. Wag-

ner, Phys. Rev. D **70**, 015007 (2004) [hep-ph/0403224].

[43] C. Pallis, Nucl. Phys. B **678**, 398 (2004) [hep-ph/0304047]. S. Profumo, Phys. Rev. D **68**, 015006 (2003) [hep-ph/0304071].

[44] S. Kraml and A.R. Raklev, Phys. Rev. D **73**, 075002 (2006) [hep-ph/0512284], S.P. Martin Phys. Rev. D **78**, 055019 (2008) [hep-ph/0807.2820].

[45] M. Drees and M.M. Nojiri, Phys. Rev. Lett. **72**, 2324 (1994) [hep-ph/9310209], Phys. Rev. D **49**, 4595 (1994) [hep-ph/9312213].

[46] S.P. Martin, Phys. Rev. D **77**, 075002 (2008) [hep-ph/0801.0237], S.P. Martin and J.E. Younkin, Phys. Rev. D **80**, 035026 (2009) [hep-ph/0901.4318], J.E. Younkin and S.P. Martin, Phys. Rev. D **81**, 055006 (2010) [arXiv:0912.4813 [hep-ph]].

[47] The ATLAS collaboration, ATLAS-CONF-2011-163; the CMS collaboration, CMS-PAS-HIG-11-032.

[48] G. Degrassi, S. Heinemeyer, W. Hollik, P. Slavich and G. Weiglein, Eur. Phys. J. C **28**, 133 (2003) [hep-ph/0212020].

[49] T. Moroi and Y. Okada, Phys. Lett. B **295**, 73 (1992). T. Moroi and Y. Okada, Mod. Phys. Lett. A **7**, 187 (1992).

[50] K.S. Babu, I. Gogoladze and C. Kolda, "Perturbative unification and Higgs boson mass bounds," hep-ph/0410085, K.S. Babu, I. Gogoladze, M.U. Rehman and Q. Shafi, Phys. Rev. D **78**, 055017 (2008) [arXiv:0807.3055 [hep-ph]].

[51] S.P. Martin, Phys. Rev. D **81**, 035004 (2010) [arXiv:0910.2732 [hep-ph]], Phys. Rev. D **82**, 055019 (2010) [arXiv:1006.4186 [hep-ph]].

[52] M. Endo, K. Hamaguchi, S. Iwamoto and N. Yokozaki, Phys. Rev. D **84**, 075017 (2011) [arXiv:1108.3071 [hep-ph]], arXiv:1112.5653 [hep-ph].

[53] J.L. Evans, M. Ibe and T.T. Yanagida, arXiv:1108.3437 [hep-ph]. T. Moroi, R. Sato and T. T. Yanagida, arXiv:1112.3142 [hep-ph].